

# ICL: Iterative closest line

## A novel point cloud registration algorithm based on linear features

Majd Alshawa\*

**ABSTRACT.** *The problem of matching 3D TLS point clouds is a necessary stage which precedes any kind of modeling in order to perfect the object's geometry and to control its accuracy. It has been studied extensively in many graphical and image-processing domains. However there is a lack of an adaptive study of this problem in the domain of laser scanning for architectural and urban purposes. Hence, our study aims to summarize the existing methods of point clouds registration. We introduce a line-based matching method which is the so-called ICL (Iterative Closest Line). Some line extraction methods required by the ICL algorithm are also presented. We compare our method to the ICP (Iterative Closest Point) one as well, which is mostly applied in the domain of point cloud and range image registration. Our method is intended to handle the special case where both of the point clouds were obtained by means of as-built topographic terrestrial laser scanner, which means that they are georeferenced and to be affined by the co-registration.*

**KEYWORDS:** *TLS, 3D matching, registration, line extraction.*

**CLASSIFICATION (COBISS):** 1.04

**UDK:** 528.2:510.5:681.7.069.24:004.352:71/72

### 1. Introduction

In order to achieve 3D architectural, urban or industrial model using the TLS point cloud, it is almost compulsory to perform multi-view scan from several stations because of the field of scanner visibility, mask conditions, object dimensions and the work conditions. Hence the 2D/3D registration is a fundamental step which precedes any posterior treatment; it can even be considered as scanning step rather than the treatment one.

The problem can be expressed in simplified technical language by overlaying an erroneous space position cloud (usually called scene or data) on another correct space position one (usually called model). Since the random instrument errors are not concerned in this approach, the resulting internal cloud geometry is stable.

This statement makes the transformation from data to model cloud a rigid one which consists of three rotations and three shifting parameters.

The problem of 3D registration is traditionally solved by adding some easily-recognized targets or spheres around the wanted object to be scanned with it. The detection of these targets or spheres in both model and data cloud allows to calculate the six parameters of rigid transformation mentioned above.

The new generation of scanner allows a setup of the scanner in a tacheometric way (back sight and front sight) in each station. This process enables one to capture a georeferenced point cloud in real time. The superposition of the resulting clouds is consequently guaranteed by previous tacheometric and topographic operations which also determinate the accu-

racy of the 3D final registration. Anyhow the 3D registration is not yet obsolete especially since the instrument setup is not always feasible.

When the scanned object includes representative geometric features, one can use them instead of external supplementary targets or spheres for achieving the 3D registration. Thus the goal of this paper is to perform free-markers registration depending on linear features as it will be explained.

The choice of linear features was privileged because of their large existence in the majority urban component. Straight lines are also useful when carrying out 2D/3D registration between a point cloud and a photogrammetric support. Nevertheless the proposed method meets its limitation when the question is to scan non-ordinary designed building.

[\*] Majd Alshawa, MSc, Photogrammetry and Geomatics Group MAP-PAGE UMR 694, Graduate School of Science and Technology (INSA), Strasbourg, France  
e-mail: majd.alshawa@insa-strasbourg.fr

After having surveyed the related work in 3D registration domain two parts will be consecrated to explain the proposed method. In the first one, three methods of linear features extraction are shown, and then two approaches of making use of these features in registration are explained.

## 2. Previous work

The general problem of 3D shape registration is largely treated in other fields of science, rather than the TLS data processing. One can therefore benefit from what has been produced in these domains like computer vision, medical images, matching 3D data with a CAD model, self localization and robotic vision.

Voting methods means that a coordinate transformation is to be done firstly then matched points from the two clouds (model-scene) are calculated. When a suggested transformation achieves a maximum score of matched point pairs, it will be a candidature for the wanted one. It can be affirmed accordingly by using an estimation method as least square adjustment. (Wolfson and Rigoutsos, 1997) used the geometric hashing as voting method to accomplish the registration. (Hecker and Bolle, 1987) adopt a method which implements Hough transform with the geometric hashing for the same purpose.

Gelfand *et al*, 2005 have introduced another category of registration methods called underlying correspondence. This class of methods focuses on the geometric characters of each point cloud rather than the number of matched points. In this category, one can find herein DARCES method (Data-Aligned Rigidity-Constrained Exhaustive Search) based on RANSAC (Random Sample Consensus) proposed by (Chen *et al*, 1999). Another underlying correspondence method is NDT (Normal Distribution Transformation) suggested by (Ripperda and Brenner, 2005). ICP (Iterative Closest Point) proposed by (Besl and McKay, 1992) which is the best known method in this category and will be discussed later on in this paper.

It can be noticed that all mentioned methods do not require a prior knowledge of any geometric features from the point cloud in opposite to another category of methods which cannot be done without extracting some geometric features or building a mesh surface of point cloud. The invariant properties of extracted features facilitate their matching in pair to pair, set in order to carry out the rigid transformation later. This gain may compensate the lost time consumed while extracting the

geometric primitives. Also, if one thinks about the use of extracted features in further modeling steps, the registration methods based on geometric primitive could be considered as an important category of registration methods. We can categorize herein the spin image method for surface matching (Johnson, 1997) and also the method based on the edges detection presented by (Sappa *et al*, 2001). (Stamos and Leordeanu, 2003) carry out a multi-scene registration depending on straight lines and plans. The same closed form solution mentioned below (4.2.1) is used when the pair-wise registration is accomplished.

Our proposed method is a feature based one, so it follows all the rules of this category starting by the features extraction stage which are straight lines in our case.

## 3. Straight line extraction

Since two points define a straight line, the number of possible trails to locate a true line representing crease or jump edge is equal to the combination  $C_n^2$ . To reduce this complexity explosion, many ergonomic algorithms are established. Three of these algorithms will be discussed below, but first of all we will restrict our search to points where a large difference in normal direction occurs. These points are »potential« to form edges in any object. RealWorks® program is capable of detecting the potential points and consequently exporting their coordinates and their normal directions in many forms. Execution time of all the three following methods improves remarkably when the last step is applied. It prevents also probable absurd solutions.

### 3.1 Incremental method

This method can be considered as projection of the method called »region growing« from 3D to 2D. Its simplicity is its main advantage. It starts by taking two points in some order and calculating the parameters of a line passing by them. A third point is then added and a line is adjusted to fit the three previous points by the least square method, which yields residuals and standard deviation estimation. The method imposes adding more and more points while the update rate of residuals is stable. When an incoherent residual occurs it should mean that the last added point does not belong to the same line. In this case the process is halted and all processed points are modeled as line segment. The process is switched then to another segment starting by the last tested point and so on until the whole po-

int cloud is tested. The criteria to accept or refuse the resulting segment will be the number of points represented by it and the standard deviation of this representation.

Two enhancements have been introduced in this basic algorithm. The first imposes sorting the cloud points based on their distances to the first point or the scanner coordinates. It is preferable in order to assist the forward marching of the algorithm. The second modification is to impose another stopping condition based on the distance between two successive points which should not exceed certain threshold.

### 3.2 RANSAC (Random Sample Consensus) algorithm

The basic form of this method (Fischler and Bolles, 1981) is used to fit a model to a set of data in presence of outliers. It has been applied widely in the computer vision and image processing fields. Nonetheless, RANSAC cannot be applied as it is to detect the edge lines because in this case the wanted output is not a single model but several lines.

A method containing RANSAC core can be stated as follows: Two points are selected randomly then the parameters of a line passing by them are calculated. The distance of all cloud points to this line are calculated and the number of those less than the proposed threshold is stored as the best number so far. Another random point pair is processed in the same way and the stored number of close points is replaced if the current number is larger. When the number of the trials proposed by RANSAC probabilistic law is reached, the stored number should represent the highest score of the modeled line. If the last number is greater than a given threshold, a line is fitted to the selected two points and all close points to their passing-by line by least square method. The last sub-set is removed from the initial point group and the method is reiterated.

Since the number of RANSAC trails is related to the size of point cloud, one should be careful to change it once a subset is taken out. This number could even be proposed by the user in such a way that the cloud is sufficiently tested in each iteration. We must accept that a certain percentage of point cloud would not be modeled whatever number of trials. Hence the stopping condition can be driven: the remaining point cloud size after several removals is less than proposed ratio of its original size.

RANSAC frequently produces a line

segment with one or two points situated on its extension since the geometric condition does not prohibit this case. A condition then verifies the adjacency of the modeled points.

### 3.3 Hough transformation

Hough transformation is a habitual method for edge detecting in 2D images. Knowing that the conversion 3D/2D is always possible by projection without losing accuracy and that the projection of the line is always a line, we can bring this method into the world of 3D terrestrial laser clouds by projecting them on xy, yz, xz or even an arbitrary plane.

This method depends on the duality between the variable and the parameter spaces. Let us be more accurate: any straight line in Oxy space has the implicit

Table 3-1. Technical specifications of the LiDAR systems			
algorithm	Incremental	RANSAC	Hough transform
Speed	-	-	+
3D/2D Functionality	+	+	-
Probability	+	--	-
Required thresholds	++	+	--
Required segment merge	--	+	+
Accuracy	+	+	-
Nombre of extracted lines	++	+	-

normal equation form:  $r = \sin\theta + y\cos\theta$  which can be read in the variable space: »infinity of (x,y) points that satisfy the equation for a unique (r,θ)«. The same equation could be read differently regarding the parameters (r,θ) as variables and the variables (x,y) as parameters: »for a unique (x,y) value, there are infinite number of (r,θ) satisfying the above equation«. Nevertheless this lecture makes the last equation

a sinusoidal one from (r,θ) point of view or more formally in the parameter space. Hence one can state that the infinite number of lines passing by a point in the variable space is presented by a sinusoid in the parameter space or in short: each point is represented by sinusoid in the parameter space. The duality variable-parameters is illustrated in Figure 3-1a and 3-1b.

Hough has noticed that when some points belong to the same line, the parameters can be retrieved from the intersection point of their sinusoid, which is the principal idea of the transformation method.

Since the representation of whole lines passing through each point is infeasible, certain discrete representation has to be considered. Hence a range of angles  $\theta \in [0, \pi]$  is proposed to accomplish the sinusoid associated to each point. We found that a range of 0.5-1° is sufficient to fulfil accuracy-processor time balance. All sinusoids are plotted in an accumulator image known (after scaling process) as Hough histogram. The next task is to find points where a substantial number of point-sinusoids intersect each other. Unfortunately, these points are not clearly marked but very often they have a butterfly (Figure 3-2). Thus the current task is to search the regional maximums in the histogram which again impose processing time and some additional thresholds definition.

The last step is to form line equations and transform them into 3D space. If

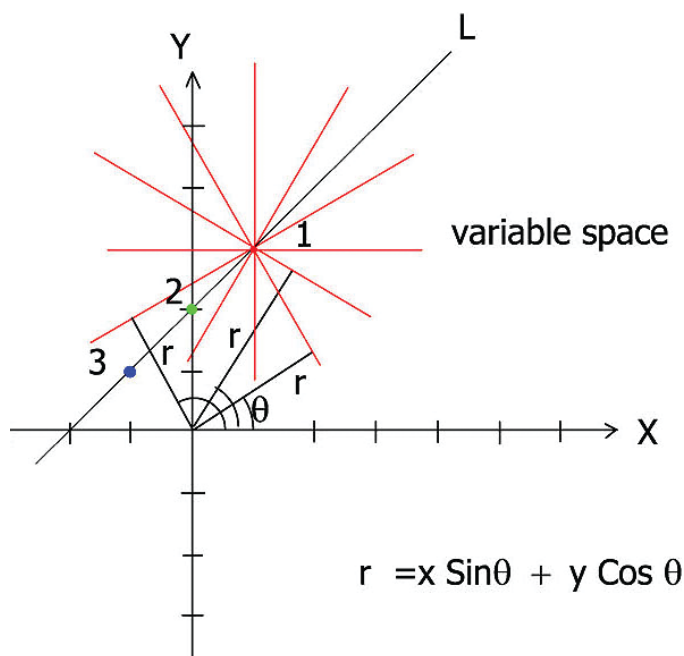


Figure 3-1a. Variable space. 1: point for whose a set of lines of different (r,θ) are shown. 2,3: two points belong to the same line L

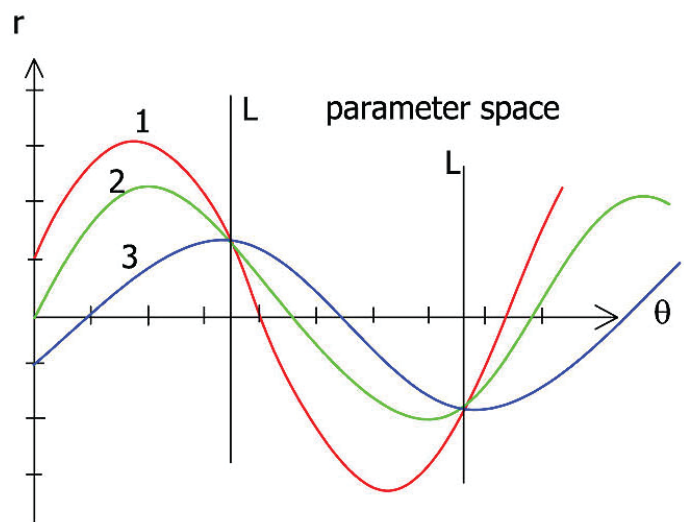


Figure 3-1b. Parameter space. 1,2,3 the sinusoids of the last three points. L: sinusoids intersection which represents the wanted common line L

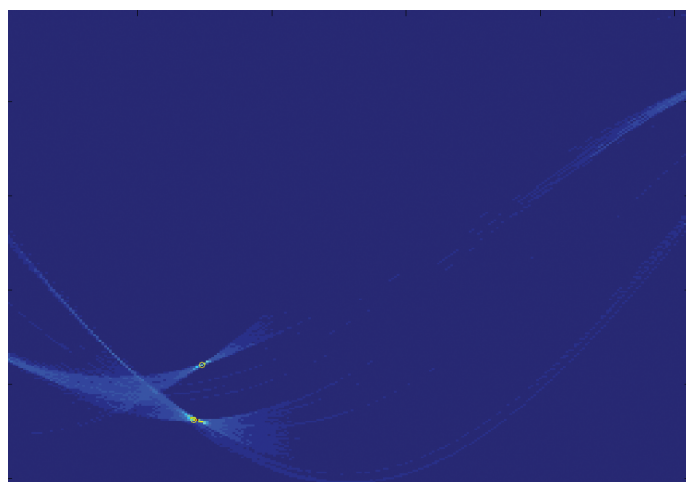


Figure 3-2. Hough histogram and its regional maxima

one searches all »close« 3D points to the found lines and then models them by the least square method, line detection accuracy will increase and the length of each segment can be determined.

### 3.4 Comparison of three methods

At this stage of research we cannot give preference to one method rather than the other. Each method has its positives and negatives (Table 3-1) and some failure cases. The major shortcoming of the incremental method is its sensitivity to the initial sequence of point cloud. For instance the incremental method is ideal for detecting the vertical edge lines for TLS scanners with vertical line of scan if no order change was made to the raw point cloud. RANSAC yields rarely different results when applied twice. Hough method meets its failure when the noise in the histogram does not allow detecting the picks in the histogram. In practice we apply a sequence of two or three methods in order to capture as many lines as possible.

Segment merge is usually carried out with respect of two conditions: the distance and the direction. This step follows line detection stage in both model and data point cloud in such manner that each of them has its own set of detected edge which is the key for starting the next step in our suggested method.

## 4. 3D registration methods

For reason of consistency, we will briefly depict the ICP method as presented in the initial paper of (Besl and Mckay, 1992) before introducing suggested methods. It will then be rather effortless to set out the principal steps of the ICL method afterwards.

### 4.1 ICP method

Let  $A$  be a set of points  $a_j$ . The distance between a point and the set  $A$  is:

$$(1) \quad d(p, A) = \min_{\{1,2,\dots,N\}} d(p, a_i)$$

The nearest point  $a_j$  to  $p$  is the one which satisfies the equality:

$$(2) \quad d(p, a_j) = d(p, A)$$

ICP method starts establishing a relation of bijection of each point of the »data« point cloud with the nearest point of the model one. (Zhang, 1992) suggests a filtering process which restricts the pairing on the overlapping zone and eliminates the

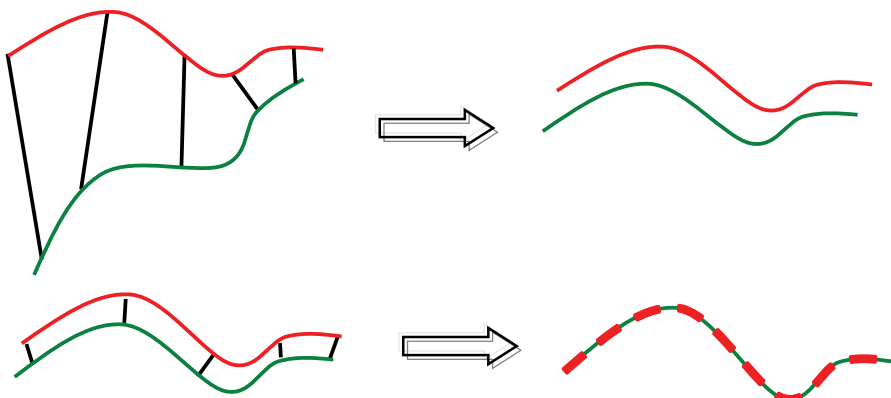


Figure 4-1. ICP coupling-transformation circle

effect of noisy data.

The next stage of ICP is to calculate the rotation matrix  $R$  and the translation vector  $T$  which are the components of the final sought rigid transformation. ICP tries to minimize the following error function:

$$(3) \quad f(R, T) = \frac{1}{N_p} \sum_{i=1}^{N_p} \| \vec{x}_i - R\vec{p}_i - \vec{T} \|^2$$

which signifies the sum of coordinate differences between each point of the »model« cloud  $x_i$  and its paired one  $p_i$  from the »data« cloud. The close form solution of equation (3) yields a provisional solution of  $R, T$  which will be applied to the »data« cloud. Another iteration of coupling-transformation is carried out starting from the recent position of data cloud (Figure 4-1). Since it has been proven that the process has to converge at some final solution, the stopping condition will be that no »significant« rigid transformation parameters are practically noticed.

### 4.2 ICL method

ICL (for Iterative Closest Line) has the same logic of ICP except that it operates lines instead of points. Two forms of this method will be presented. The one differs from the other in the second process stage which is the rigid transformation. Nevertheless the core of the two forms is line pairing from both point clouds. The condition of line coupling is the distance between them in the early iteration of the process. When the method begins converging, one can introduce a direction condition; the coupled lines have to be »parallels« within certain threshold. It is obvious that the number of coupled line  $N$  pairs is equal to minimum number of extracted line in both data and model cloud. Once the lines are coupled the calculation of rigid transformation can be started:

#### 4.2.1 The ICP Form

Firstly, lines have to be presented by a direction vector  $v$  and some point coordinates

$p$  the superscript 'm', 'd' will denote the model and the data cloud respectively. The rotation matrix can be concluded from lines direction only when minimizing the following function:

$$(4) \quad Err(R) = \sum_{i=1}^N \| v_i^m - Rv_i^d \|^2$$

As in the ICP method, the solution of this function is of closed form. For doing so, the two following means are defined:

$$(5) \quad \mu_v^m = \frac{1}{N} \sum_{i=1}^N v_i^m, \mu_v^d = \frac{1}{N} \sum_{i=1}^N v_i^d$$

Cross covariance matrix of the two data sets is:

$$(6) \quad \sum_{v^m, v^d} = \frac{1}{N} \sum_{i=1}^N (v_i^m v_i^{dT} - \mu_v^m \mu_v^{dT})$$

The cyclic components of the anti-symmetric matrix  $A_{ij}$  are used to formulate the vector called  $\Delta$  used by its turn to formulate the matrix  $Q(\sum)$ :

$$(7) \quad A_{ij} = \left( \sum_{v^m, v^d} - \sum_{v^m, v^d} \right)_{ij}$$

$$\Delta = [A_{23}, A_{31}, A_{12}]$$

$$Q(\sum) = \begin{bmatrix} tr(\sum_{v, v'}) & \Delta^T \\ \Delta & \sum_{v, v'} - \sum_{v, v'}^T - tr(\sum_{v, v'}) I_3 \end{bmatrix}_{4 \times 4}$$

It was proven that the vector of normalized eigenvector of the matrix (7) represents the optimal rotation quaternion  $\vec{q}_R [q_0 q_1 q_2 q_3]$ . Euler angles rotation matrix is given by:

$$(8) \quad R(\vec{q}_R) = \begin{bmatrix} q_0^2 + q_1^2 - q_2^2 - q_3^2 & & & \\ 2(q_2 q_1 + q_0 q_3) & & & \\ 2(q_3 q_1 - q_0 q_2) & & & \\ & & & & \end{bmatrix}$$

$$\begin{bmatrix} 2(q_1 q_2 - q_0 q_3) & 2(q_1 q_3 + q_0 q_2) \\ q_0^2 - q_1^2 + q_2^2 - q_3^2 & 2(q_2 q_3 - q_0 q_1) \\ 2(q_3 q_2 - q_0 q_1) & q_0^2 - q_1^2 - q_2^2 - q_3^2 \end{bmatrix}$$

Once the rotation matrix is calculated, it can be used to find the shifting vector  $T = (T_x T_y T_z)^T$ . Let us take two random points ( $a^m_i, a^d_i$ ) belong to the  $i^{th}$  line ( $v^m_i, p^m_i$ ) detected in the model cloud; these points fulfil the triple of equation:

$$(9) \quad \begin{aligned} a_{1}^m &= p_{i}^m + t_{1}^m v_{i}^m \\ a_{2}^m &= p_{i}^m + t_{2}^m v_{i}^m \end{aligned}$$

They have two homogenous points on the paired line  $i$  in the data cloud which satisfies to the triplet of equation:

$$(10) \quad \begin{aligned} a_{1}^d &= p_{i}^d + t_{1}^d v_{i}^d \\ a_{2}^d &= p_{i}^d + t_{2}^d v_{i}^d \end{aligned}$$

The relation between both lines yields the following equations:

$$(11) \quad \begin{aligned} a_{1}^d &= R a_{1}^m + T \\ a_{2}^d &= R a_{2}^m + T \\ p_{i}^d + t_{1}^d v_{i}^d &= R(p_{i}^m + t_{1}^m v_{i}^m) + T \\ p_{i}^d + t_{2}^d v_{i}^d &= R(p_{i}^m + t_{2}^m v_{i}^m) + T \end{aligned}$$

This system of six equations has seven variables: three translations and four variables ( $t_{1}^m, t_{2}^m, t_{1}^d, t_{2}^d, T_x, T_y, T_z$ ). Thus another pair of points is needed for accomplishing the calculation. When we have two or more pairs of lines, the over determined system (11) has to be solved by the least square adjustment method.

#### 4.2.2 Alternative form

This form is more comprehensible for whomever is not familiar with the close-form of solution. It depends upon the basic idea suggested by (Habib and Ghanma, 2004) where they integrate a point cloud with a 3D photogrammetric model by co-joining the extracted linear features.

In the Figure 4-2, the two points  $A, B$  represent a segment of the model cloud. 1 and 2 define the paired line segment from the data cloud.

The rigid transformation for the segment 1, 2 is given by the equations :

$$(12a) \quad \begin{bmatrix} T_x \\ T_y \\ T_z \end{bmatrix} + R \begin{bmatrix} X_1 \\ Y_1 \\ Z_1 \end{bmatrix} = \begin{bmatrix} X_A \\ Y_A \\ Z_A \end{bmatrix} + \lambda_1 \begin{bmatrix} X_B - X_A \\ Y_B - Y_A \\ Z_B - Z_A \end{bmatrix}$$

$$(12b) \quad \begin{bmatrix} T_x \\ T_y \\ T_z \end{bmatrix} + R \begin{bmatrix} X_2 \\ Y_2 \\ Z_2 \end{bmatrix} = \begin{bmatrix} X_A \\ Y_A \\ Z_A \end{bmatrix} + \lambda_2 \begin{bmatrix} X_B - X_A \\ Y_B - Y_A \\ Z_B - Z_A \end{bmatrix}$$

where  $\lambda_1, \lambda_2$  are two scale factors express the slide of one segment on the other. Subtraction of equation (12b) from (12a) gives:

$$(13) \quad \begin{bmatrix} X_B - X_A \\ Y_B - Y_A \\ Z_B - Z_A \end{bmatrix} = \lambda R \begin{bmatrix} X_2 - X_1 \\ Y_2 - Y_1 \\ Z_2 - Z_1 \end{bmatrix}$$

$\lambda = 1/(\lambda_2 - \lambda_1)$  is a new scale factor, which could be eliminated by dividing the first and the second line by the third:

$$(14) \quad \begin{aligned} \frac{X_B - X_A}{Z_B - Z_A} &= \frac{R_{11}(X_2 - X_1) + R_{31}(X_2 - X_1) + R_{12}(Y_2 - Y_1) + R_{13}(Z_2 - Z_1) + R_{32}(Y_2 - Y_1) + R_{33}(Z_2 - Z_1)}{R_{31}(X_2 - X_1) + R_{32}(Y_2 - Y_1) + R_{33}(Z_2 - Z_1)} \\ \frac{Y_B - Y_A}{Z_B - Z_A} &= \frac{R_{21}(X_2 - X_1) + R_{22}(Y_2 - Y_1) + R_{23}(Z_2 - Z_1) + R_{32}(Y_2 - Y_1) + R_{33}(Z_2 - Z_1)}{R_{31}(X_2 - X_1) + R_{32}(Y_2 - Y_1) + R_{33}(Z_2 - Z_1)} \end{aligned}$$

The last double equation in three variables is not sufficient for accomplishing the solution, so at least one equation of second line pair is needed. Usually we use all the available pairs from the previous coupling to process them by the least square adjustment method.

After obtaining the rotation matrix, one can substitute its value into the equation (12a) for the first point:

$$\begin{bmatrix} T_x \\ T_y \\ T_z \end{bmatrix} + \begin{bmatrix} x_1 \\ y_1 \\ z_1 \end{bmatrix} = \begin{bmatrix} X_A \\ Y_A \\ Z_A \end{bmatrix} + \lambda_1 \begin{bmatrix} X_B - X_A \\ Y_B - Y_A \\ Z_B - Z_A \end{bmatrix}$$

where

$$(15) \quad \begin{bmatrix} x_1 \\ y_1 \\ z_1 \end{bmatrix} = R \begin{bmatrix} X_1 \\ Y_1 \\ Z_1 \end{bmatrix}$$

To eliminate the scale factor we have to divide into the third line as well:

$$(16) \quad \begin{aligned} \frac{X_B - X_A}{Z_B - Z_A} &= \frac{T_x + x_1 - X_A}{T_z + z_1 + Z_A} \\ \frac{Y_B - Y_A}{Z_B - Z_A} &= \frac{T_y + y_1 - Y_A}{T_z + z_1 + Z_A} \end{aligned}$$

In the same way point 2 generates the same equations. The solution of all the paired lines equations by the least square adjustment gives the shifting vector directly.

It is obvious from the two forms of ICL that two couples of non-coplanar

lines are sufficient for carrying out the rigid transformation; nevertheless the growth of line number makes the solution more robust and eliminates eventual errors. Both forms of solution reflect the separation of rigid transformation solution into a non-linear stage stating the rotation and a linear stage expressing the shift. Nonetheless ICP form saves processor time needed by the iterative solution of the second form when computing rotation parameters.

## 5. Test results

The chosen application herein is the documentation scan of the »Pontonniers international high school« in Strasbourg. This scan respects the survey workflow (Hanke *et al.*, 2006). Hence, already registered point clouds allow comparing the result of ICL registration with data from the topographic methods. Figure 5-1a shows the superposition of two point clouds in Realworks® according to the scanner attitude and position determined by posterior topographic operations. Table 5-1 summarizes the main characteristic of both point clouds acquisition and treatment.

A combination of successive RAN-SAC and incremental method is applied in order to obtain the maximum number of lines. The thresholds shown in Table 5-1 have been selected with respect to the scan resolution and density. The result of coupling by using previous conditions can be controlled visually by the user (Figure 5-1b). One can see that a more tolerant threshold yields more lines but at the cost of loosing the precision which affects the next step severely.

To accomplish the pairing stage of

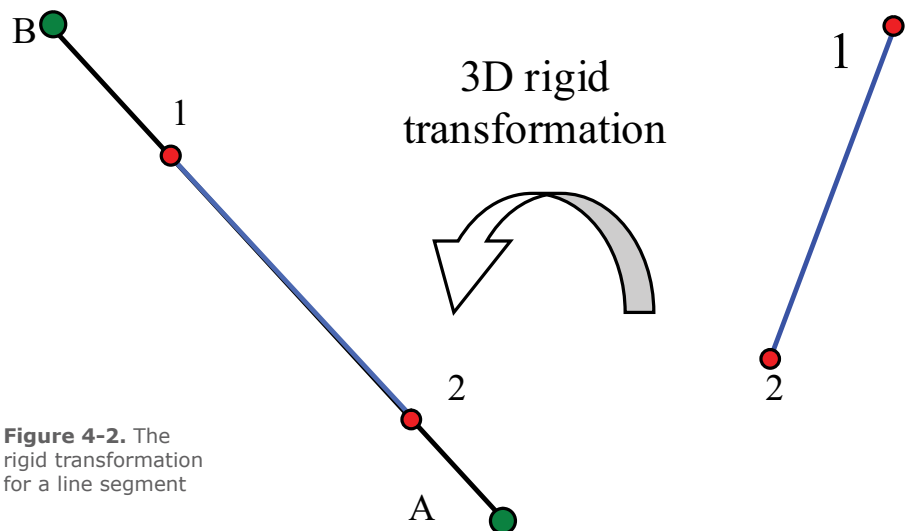


Figure 4-2. The rigid transformation for a line segment

ICL, we supposed that the final pairing distance threshold is 60 mm and the direction one is 0.5.gon. 13 lines remain to contribute in the afterwards rigid transformation calculation. The reason behind this fall is the modeling of the visible edges of cylindrical tiles used for covering roofs seals as invariant lines. Knowing that the boards of a cylinder seen from different points of view are not the same, two lines are generated which are not supposed to be the same. This error is eliminated by the direction and distance filter proposed by the pairing processes.

Table 5-2 shows the results of the application of both ICL forms.

Although the tiny observed values (the two point clouds supposed to be already correctly overlapped), one can see that the form ICP tries to solve the problem of registration in its last steps by rotation when the form alternative accomplishes that by translation. This observation can be interpreted by the accuracy of the iterative and the closed form of the least square adjustment especially when it is a question of miniature displacements. If one admits that a small rotation about a frame situated fairly far can be translated as a linear shift, the two solutions will be fairly equivalent. It is enough to compute the effect of the given rotations around the frame axis at the centre of the cloud and then to add it to the calculated translations.

The coordinate difference between the automatic overlapping of the two point clouds due to the acquisition process and ICL registration can be explained by the following factors:

1. The imperfection of the prior surveying works.
2. TLS random errors as eccentricity and bubble errors.
3. TLS instrumental errors which affect the measured range and angles.
4. TLS environmental and object related errors which affect the laser beam deflection.

We can compare ICL registration results with the first error in this context of work especially because the second error is unknown and the rest are insignificant when compared to the first one. More particularly, ICL results are comparable with the accuracy of R14 which was the origin of the data cloud (Table 5-1). We can see obviously that the form ICP yields more accurate results (difference of 2-3 mm) than the alternative method (difference of 4-8 mm). Processor time saving is another factor which makes us advise the use of the form ICP of ICL.

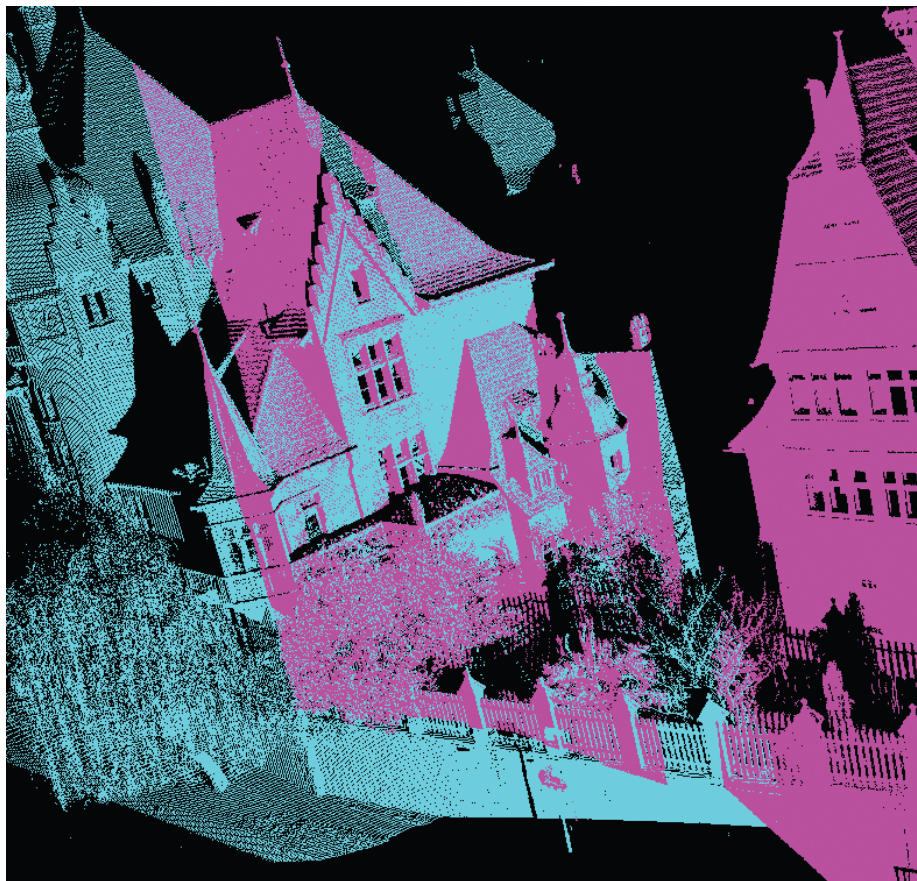


**Figure 5-1a.** Overlap zone between the two clouds. b) The potential points and the extracted edge lines

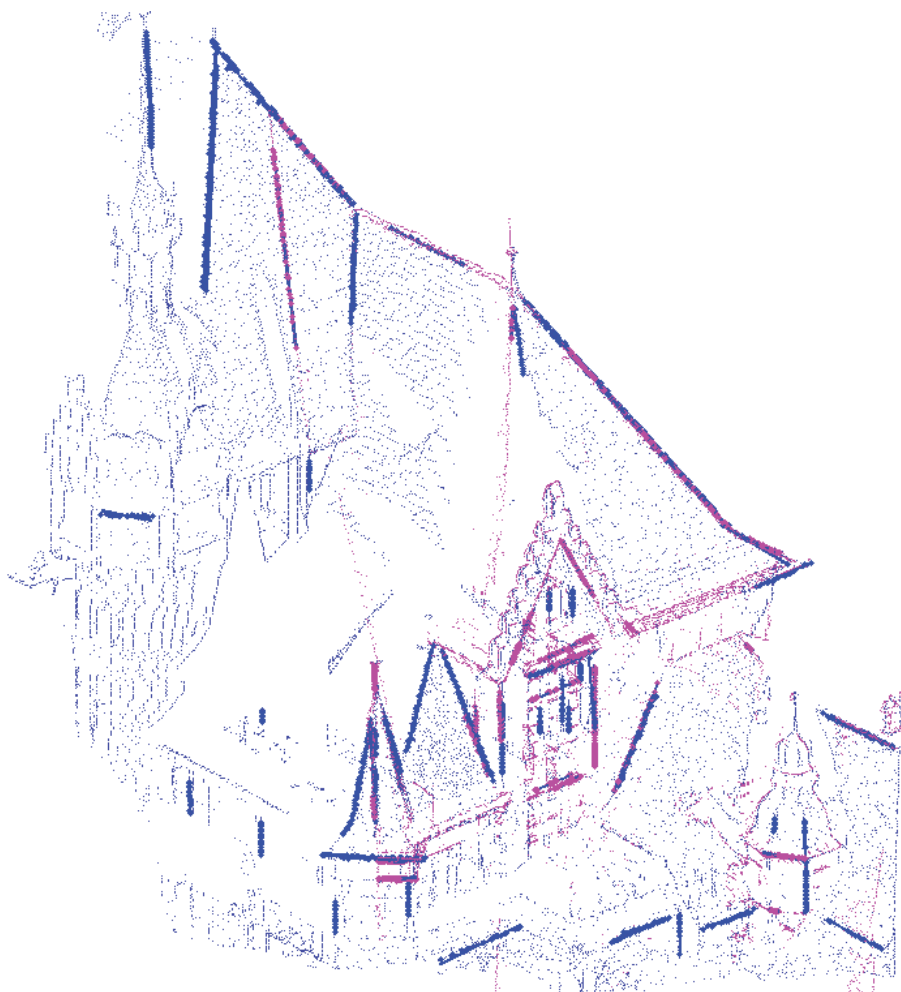


**Figure 5-1b.** Overlap zone between the two clouds. b) The potential points and the extracted edge lines

**Table 5-1. Acquisition and processing parameters**

Scan origin	I13 (model)	R14 (data)
X,Y,Z accuracy resp. (cm)	0.4, 0.2, 0.3	-1.1, 1, -0.9 resection by scanner itself
Linear resolution	50 mm at 60 m	30 mm at 60 m
Points number	292706	601952
Potential points	15401	9527
Number threshold (Ransac+ Incremental)	20	30
Distance threshold	35 mm	20 mm
Extracted lines	33	48

**Table 5-2. The rigid transformation components when registering the two points cloud.  $\sigma$  : The standard deviation of the estimation. »Total« is the effect of the calculated rotations at a distance of 50 m plus the shift as well**

ICL ( ICP form)					
axis	Rotation mGon	$\sigma$ mGon	Shift (cm)	$\sigma$ (cm)	Total (cm)
x	12	0.3	0.2	0.2	1.1
y	-5	0.3	-0.8	0.2	-1.2
z	11	0.2	0.3	0.2	1.2
RMS	RMS : 0.5 mGon		RMS : 0.2 cm		0.2
ICL (alternative form)					
axis	Rotation mGon	$\sigma$ mGon	Shift (cm)	$\sigma$ (cm)	Total (cm)
x	2	0.2	1.8	0.3	1.8
y	-4	0.2	-1.5	0.3	-1.7
z	9	0.2	0.6	0.2	1.3
RMS	RMS : 0.4 mGon		RMS : 0.4 cm		0.4

## 6. Conclusion

As we have seen in this approach, the edge lines are firstly detected and then used for the registration. We are yet far from possessing a global edge-detection algorithm which digitizes all lines in a point cloud. Hence, we still use a combination of the three suggested methods to collect the maximum line segments and then we try to merge the needed segments. The ICL method's final accuracy depends upon the line detection's accuracy which is probably the major shortcoming of the method. Line directions affect directly the rotation components of the rigid transformation which affect in turn the sifting component's computation. The use of large thresholds produces a greater number of lines but they are less accurate, while the use of strict threshold produces a more accurate solution but it has less redundancy. However, a careful line detection controlled by the user yields a final matching accuracy better than the scan linear resolution which is sufficient for further application.

## 7. Future work

Until now, the tests that we have done confirm only the scanner accuracy and help us control the previous topographic work. We still need some other tests to prove the method efficiency in the general case. In our future work we will, hopefully, enhance some aspects of general 3D matching as:

1. Straight lines extraction as contours of planes.
2. Use of other geometric features like curves and planes
3. Use of other geometric relations like orthogonality, parallelism and the intersection by known angles.
4. Extension of the method in order to be able to trait multiple point clouds simultaneously without accumulating the cloud-to-cloud registration error.

## References

- Besl, P. J., and McKay, N. D. (1992): A method for registration of 3-D shapes. IEEE Trans. on Pattern Analysis and Machine Intelligence, vol: 14, 2, pp. 239-256.
- Chen, C.S., Hung, Y.P., and Cheng, J.B. (1999): Ransac-based DARCES: A new approach to fast automatic registration of partially overlapping range images. IEEE Transactions on Pattern Analysis and Machine Intelligence, vol: 21(11) pp. 1229-1234.
- Hecker, Y.C., Bolle, R.M. (1994): On geometric hashing and the generalized Hough transform. IEEE transactions on Systems, Man and Cybernetics, vol: 24, pp. 1328-1338.
- Wolfson, H. J., and Rigoutsos, I. (1997): Geometric hashing: an overview. IEEE Computational Science & Engineering, vol: 13, pp. 10-21.
- Zhang, Z. (1992): Iterative point matching for registration of free-form curves and surfaces. International Journal of Com-

puter Vision, vol: 13, 2, pp. 119-152.

- Fischler, M. A., and Bolles. R. C., (1981): Random Sample Consensus: A Paradigm for Model Fitting with Applications to Image Analysis and Automated Cartography. Comm. of the ACM, Vol 24, pp. 381-395.
- Gelfand, N., Mitra, N.J., Guibas L.J., and Pottmann H. (2005): Robust Proceedings of Symposium on Geometry Processing, pp.197-206
- Habib, A. F, Ghanma, M. S., and Tait, M. (2004): Integration of lidar and photogrammetry for close range applications. Proceedings of the ISPRS Geo-Image-ry Bridging Continents.
- Hanke K., Grussenmeyer P., Grimm-Pitzinger, A. and Weinold Th. (2006): First experiences with the Trimble GX scanner. Proceedings of the ISPRS commission V symposium »Image Engineering and Vision Metrology«.
- Ripperda, N. and Brenner, C. (2005): Marker-free registration of terrestrial laser scans using the normal distribution transform. Proceedings of the ISPRS working group V/4 workshop, 3D-ARCH.
- Sappa, A., Restrepo-Specht, A., and Devy. M. (2001): Range image registration by using an edge based representation. Proceedings of the 9th International Symposium on Intelligent Robotic Systems.
- Stamos, I. and Liordeanu, M. (2003): Automated feature-based range registration of urban scenes of large scale. In Proc. CVPR, IEEE, Madison, Wisconsin, June 16-22, vol. II, pp. 555-561. 